JMEPEG (2006) 15:575-580
DOI: 10.1361/105994906X124569

1059-9495/$19.00

Constitutive Model of Micromechanical Damage to Predict Reduction in Stiffness of a Fatigued SMC Composite

A. Ben Cheikh Larbi, K. Sai, H. Sidhom, and D. Baptiste

(Submitted November 20, 2004; in revised form December 20, 2005)

Elastic behavior of sheet molding compound (SMC) composites with a given orientational distribution of fibers under cyclic loading is investigated herein. Fatigue tests were carried out over various strain ranges. During each test, evolution of Young's modulus was measured and the composite was analyzed using scanning electron microscopy. Observations revealed the principal form of degradation to be matrix fiber debonding. A constitutive model that takes into account the reduction of overall elastic properties, i.e., Young's modulus, was developed. This model uses a Mori-Tanaka mean field approach coupled with a micromechanical damage law. The energetic failure criterion and the failure probability are functions of local shear and normal stresses calculated at each point of the interface of each fiber family. A procedure for identifying the most appropriate material parameters is described in detail. The proposed model agrees well with the experimental results.

Keywords Eshelby, fatigue damage, interfacial failure, micromechanical law, Mori-Tanaka, parameter identification, sheet molding compound (SMC) composite

1. Introduction

In recent years, composite materials have become highly attractive for structural applications, due both to their technical merit and their economic potential. One example is the sheet molding compound (SMC), which, due to its esthetic, electrical and mechanical properties, finds use in a wide range of applications. Short glass fibers (20-30 mm in length) are randomly distributed in a polyester resin. This process introduces a scatter of micromechanical parameters of the fibers, and the behavior of the composite is very sensitive to the volume fraction of fibers, the distribution of their orientations, and the aspect ratio of the reinforcement. It is important to be able to predict the mechanical behavior and damage behavior of the SMC in relation to the properties of the microstructure. Mechanical behavior of SMC has been also investigated (Ref 1-3). In previous works (Ref 4, 5), debonding was observed to influence the macroscopic properties of composite materials. Analytical and experimental models of cumulative damage were developed to predict the lifespan of the structures in the composites (Ref 6-13).

The effect of matrix degradation and interfacial debonding on stiffness reduction in a random discontinuous fiber composite was studied by Meraghni et al. (Ref 14). To identify damage mechanisms, they carried out both microscopic observations and acoustic emission analysis.

Lee et al. (Ref 15) developed and analyzed a micromechanical model for predicting bridging laws of short fiber composites with deterministic length. Similar models were proposed by Maalej (Ref 16), who took into account the variability of fiber strength.

The works of Guo et al. (Ref 17-21) then proposed a constitutive model for micromechanical damage of SMC composite under monotone loading. Le Pen et al. (Ref 22) developed a Mori-Tanaka model that included a law for fiber-breaking damage in fatigue of Al-Al_2O_3 composites.

The model proposed in this paper draws its inspiration from this class of models and, in addition, takes into account the cyclic damage of the SMC composite. The elementary physical mechanisms of damage must be well identified, and we describe them by local criteria on the microscopic level (i.e., on the scale of the fiber). In the present work, an energetic failure criterion is introduced into the micromechanical model. Macroexperimental fatigue tests were carried out to determine this criterion.

The aim of this work is to describe the reduction in stiffness of the composite as a function of the number of cycles. The full optimization procedure requires the analysis of thousands of cycles and thus rapidly becomes prohibitive. To avoid this, the so-called "cycle jump technique" developed by Lesne (Ref 23) was used. In Section 2, the material characteristics and experimental procedure are presented. Section 3 is devoted to the model used. The main constitutive equations of the model are described, and then the algorithm and numerical implementation are shown. The experimental results related to the damage mechanism are discussed in Section 4, where the identification of the material parameters and a comparison between experimental results and numerical simulation are also presented.

A. Ben Cheikh Larbi and **H. Sidhom**, Laboratoire de Mécanique Matériaux et Procédés, Ecole Supérieure des Sciences et Techniques de Tunis, Tunisia; **K. Sai,** Unité de Génie de Production Mécanique et Matériaux, Ecole Nationale d'Ingénieurs de Sfax, 5, Av Taha Hussein B.P. 56 1008 Tunis, Tunisia; and **D. Baptiste**, Laboratoire Ingénierie des Matériaux, Ecole Nationale Supérieure d'Arts et Métiers, UMR CNRS 8006, 151, Boulevard de l'Hôpital, 75013 Paris, France. Contact e-mail: ahmed.ben-cheikh@laposte.net.

2. Materials and Methods

The material investigated herein is an SMC composite. The microstructural nature of this material is as follows. The matrix consists of a mixture of polyester resin and a mineral charge of $CaCo_3$ particles, between 2 and 30 μm in size. Reinforcement, introduced as bundles with a nominal mass fraction of 42%, are randomly oriented, short fiber-glass fibers, 25 mm in length. The SMC composite used is Inoplast (supplied by Marwe Composites, France) in the form of a thin sheet, 2.6 mm thick. To analyze the microstructure of the fiber bundles, some specimens were sectioned along three perpendicular directions. In a given plane, the orientation distribution was obtained by scanning electron microscopy (SEM) coupled with image analysis. A low orientation of fibers in the matrix is noted. As a result of these experimental investigations, the fiber orientation θ is obtained with:

$$\theta = \arcsin(a/b) \quad \text{(Eq 1)}$$

The orientation distribution of fibers in the SMC matrix was obtained by Keyvani (Ref 24). The volume fraction of fibers with the same orientation is θ_i, and consequently the orientation distribution is given by:

$$\frac{f_i}{f} = \frac{1}{nf}[1 + \alpha \cos(2\theta^i - \pi)] \quad \text{(Eq 2)}$$

where f_i is the volume fraction of fibers directed according to the angle θ_i, f is the total volume fraction of fibers, nf is the total number of fiber families, and α is the percentage of disoriented fibers ($\alpha = 14\%$).

The main mechanical characteristics of the SMC composite are shown in Table 1.

A typical tensile test of the SMC composite is shown in Fig. 1. Pure elastic behavior is observed up to a stress level of 20 MPa, above which elastic behavior with damage is seen.

To identify the damage mechanisms of the SMC composite under cyclic loading, fatigue tests combined with microstructural SEM analysis were carried out. Four cyclic tension-compression tests under strain-controlled loads were performed on an MTS (Material Tests Systems, Eden Prairie, MN) fatigue machine. The adopted ratio between the maximum and minimum strain levels was $R_\varepsilon = 0.1$, and the test frequency was 5 Hz. Various levels of loading, quantified in amplitude of deformation, were imposed: $\Delta\varepsilon_1 = 0.60\%$, $\Delta\varepsilon_2 = 0.72\%$, $\Delta\varepsilon_3 = 0.80\%$, $\Delta\varepsilon_4 = 0.87\%$. Four specimens were tested for each condition. During each test, evolution of the Young's modulus with the number of cycles was measured, and SEM observations were made of specimens from interrupted tests

The fatigue tests were carried out to study the reduction in stiffness for the various imposed amplitudes of deformation. Figure 2 shows evolution of the ratio E/E_0 with N for each level of loading, where E_0 is the initial Young's modulus and E is the Young's modulus at cycle N. A similar tendency was observed over each of the four ranges of strain. A very slow linear decrease of the Young's modulus was observed over the first 90% of the life of the SMC. This was followed by a rapid decrease in the modulus during the last 3 to 5% of the life before fracture.

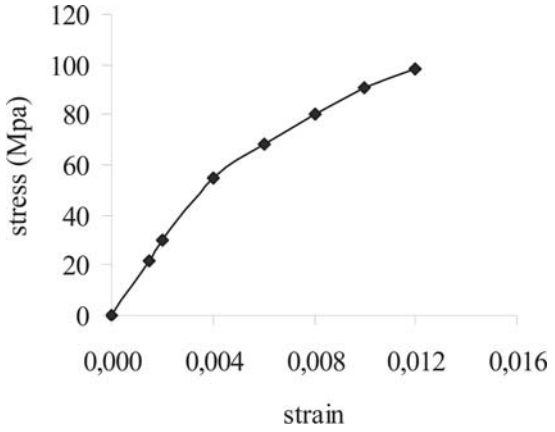

Fig. 1 Typical tensile curve of SMC composite

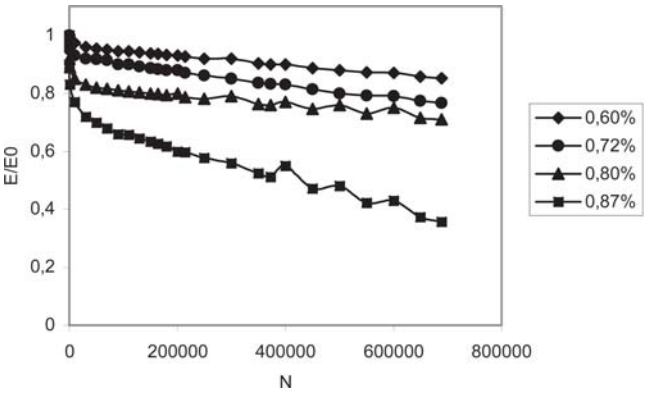

Fig. 2 Evolution of stiffness reduction with number of cycles

Table 1 Mechanical properties of materials studied

	E, GPa	ν	σ_u, MPa
Polyester matrix	3.5	0.35	50
Glass fibers	72–74	0.28	1500
SMC 42 Composite	15–16	…	128

The reduction in stiffness appears to be more marked when the amplitude of deformation increases. This phenomenon can be explained at the microstructural level by the mechanism of degradation. SEM observations of specimens prepared from interrupted fatigue tests showed that the degradation occurs in two stages. First, microscopic fissure start to appear on the level of the interface fiber matrix. The initiation of these interfacial microscopic fissures is independent of the fiber orientation in the matrix and involves a reduced number of fibers. Second, the microscopic fissures propagate and coalesce so that gradually the fibers become locked to one another. The fissures crossing the matrix and separating the locks of fibers circumvent the chalk particles and remain overall perpendicular to the direction of loading (Fig. 3).

3. Numerical Modeling

3.1 Constitutive Equations

Basic equations used the micromechanical model to determine composite stiffness, and equations for the local stresses

on the fiber-matrix interface are also based on the approach of Mori and Tanaka (Ref 25). The mathematical treatment of such composite is obtained by considering the stiffness of either the matrix or the fiber to be isotropic.

Overall stress is respectively explained in relation to the matrix strain and the overall strain. With the help of Eshelby's theory (Ref 26, 27) for an ellipsoidal inclusion defined by an aspect ratio (length/diameter), the composite stiffness tensor $\tilde{\tilde{L}}_{comp}$ is given by:

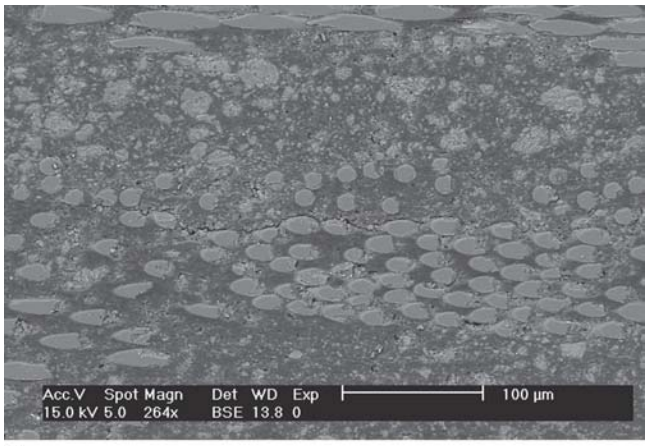

(a)

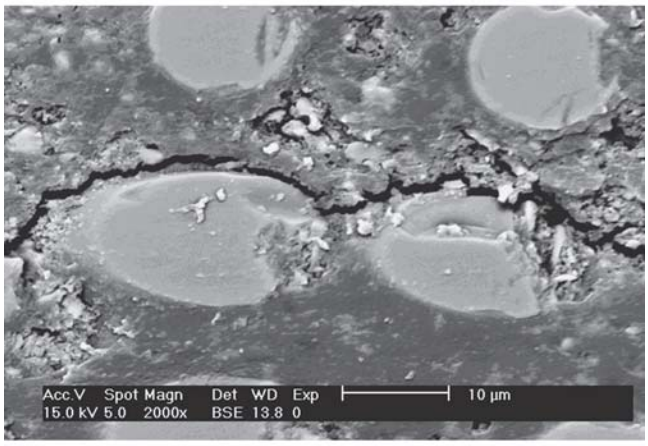

(b)

Fig. 3 Damage evolution for fiber family perpendicular to the load ($\theta = 90°$)

$$\tilde{\tilde{L}}_{comp} = \tilde{\tilde{L}}_m:[\tilde{\tilde{I}} + \tilde{\tilde{Q}}:(\tilde{\tilde{I}} + \tilde{\tilde{H}})^{-1}]^{-1} \quad \text{(Eq 3)}$$

in which $\tilde{\tilde{I}}$ represents the fourth-rank identity tensor. $\tilde{\tilde{H}}$ and $\tilde{\tilde{Q}}$ are deduced from stiffness tensor of the matrix and from the stiffness tensor of any fiber i:

$$\tilde{\tilde{H}} = \sum_i \frac{f_i}{f}(\tilde{\tilde{S}}^i - \tilde{\tilde{I}}):\tilde{\tilde{Q}}^i \quad \text{(Eq 4)}$$

$$\tilde{\tilde{Q}} = \sum_i \frac{f_i}{f}\tilde{\tilde{Q}}^i \quad \text{(Eq 5)}$$

$$\tilde{\tilde{Q}}^i = [\tilde{\tilde{L}}^m + (\tilde{\tilde{L}}^i - \tilde{\tilde{L}}^m):\tilde{\tilde{S}}^i]^{-1}:(\tilde{\tilde{L}}^m - \tilde{\tilde{L}}^i) \quad \text{(Eq 6)}$$

where $\tilde{\tilde{S}}^i$ is the Eshelby tensor of the ith fiber family, which depends on the matrix mechanical characteristics. $\tilde{\tilde{L}}^m$ and $\tilde{\tilde{L}}^i$ are the stiffness tensor for the matrix and the fiber, respectively. The above theory leads to the expression of local stress tensor $\tilde{\boldsymbol{\sigma}}^i$ in the inclusion:

$$\tilde{\sigma}^i = \tilde{\tilde{L}}^m:(\tilde{\tilde{I}} + \tilde{\tilde{H}}^i):(\tilde{\tilde{I}} + \tilde{\tilde{H}}^i)^{-1}:\tilde{\tilde{E}}_0 \quad \text{(Eq 7)}$$

where $\tilde{\tilde{E}}_0$ denotes the uniform macrostrain tensor. These tensors are all expressed in the macroscopic principal axes of the composite plate.

The interfacial failure criterion is generally expressed as a function of both normal stress σ and shear stress τ at the interface. These local stresses are obtained by projection of the local stress tensor $\tilde{\boldsymbol{\sigma}}^i$ in the local basis of the fiber (Fig. 4).

A number of studies used the Coulomb criterion, in which a friction coefficient at the fiber/matrix interface is introduced. In this study, the adopted criterion takes into account of both interfacial stress state and the number of loading cycles N. Hence an energetic criterion is written in a statistical form:

$$\left(\frac{\sigma}{A/(B+N)}\right)^2 + \left(\frac{\tau}{C/(D+N)}\right)^2 = 1 \quad \text{(Eq 8)}$$

In this last expression, the ratios A/B and C/D represent the normal and shear stresses, respectively, for which the criterion is satisfied during the first cycle. This criterion is chosen to describe decrease of the interfacial strength with the number of

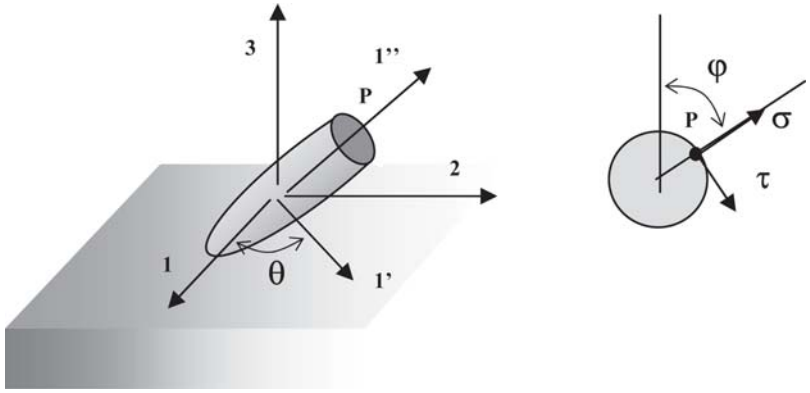

Fig. 4 Local and composite basis

cycles. Using this criterion, the interfacial failure probability for each fiber orientation family θ^i is given by:

$$Pr(\theta^i) = 1 - \exp\left[-\left(\left(\frac{\sigma}{A/(B+N)}\right)^2 + \left(\frac{\tau}{C/(D+N)}\right)^2\right)^m\right] \quad \text{(Eq 9)}$$

where m is a material parameter related to the scatter of microstructure. Normal stress σ and shear stress τ depend on the macroscopic stress and fiber orientation, volume fraction, aspect ratio of the fiber, elastic properties of the matrix, and the fiber.

In these conditions, the orientation distribution of fibers varies with the number of cycles. After the interfacial debonding between fibers and the matrix, the damaged fibers are substituted by the matrix (Ref 17). The expression of localization tensors given in Eq 4 and 5 becomes:

$$\tilde{\tilde{\boldsymbol{H}}} = \sum_i \frac{f_i}{f}[1 - Pr(\theta^i)](\tilde{\tilde{\boldsymbol{S}}}^i - \tilde{\tilde{\boldsymbol{I}}}):\tilde{\tilde{\boldsymbol{Q}}}^i \quad \text{(Eq 10)}$$

$$\tilde{\tilde{\boldsymbol{Q}}} = \sum_i \frac{f_i}{f}[1 - Pr(\theta^i)]:\tilde{\tilde{\boldsymbol{Q}}}^i \quad \text{(Eq 11)}$$

The stiffness tensor of SMC can finally be computed for each cycle. This allows the evolution of the reduction in Young's modulus to be obtained as a function of the number of cycles.

3.2 Implementation of the Method

The equations described in the last section will either be used in simulation analysis or integrated into an optimization code. Figure 5 shows the algorithm of this method. The matrix and fiber characteristics are used to calculate tensors $\tilde{\tilde{\boldsymbol{H}}}^i$ and $\tilde{\tilde{\boldsymbol{Q}}}^i$ for each family of fiber in the case of safe material (without any damage). At the same time, the orientation distribution is initialized.

For the first cycle, $\tilde{\tilde{\boldsymbol{H}}}$ and $\tilde{\tilde{\boldsymbol{Q}}}$ are calculated with an interfacial failure probability equal to zero for all fibers. Furthermore, interfacial failure probability founded at cycle N will be introduced in Eq 10 and 11 to compute tensors $\tilde{\tilde{\boldsymbol{H}}}$ and $\tilde{\tilde{\boldsymbol{Q}}}$ at cycle $N + 1$.

Normal and shear stresses are obtained at the interfacial fiber matrix. For a given orientation, the considered interfacial failure criterion is the maximum one all around the fiber.

A method referred to as the "cycle jump technique" (Ref 23) is used to accelerate calculation. The key of this method, initially developed for viscoplastic structure calculations involving large number of cycles, is the use of an automatic step control. Accordingly, when possible, a certain number of cycles are jumped.

3.3 Parameter Identification

To identify the material parameters, the optimization code SIDOLO developed by Pilvin (Ref 28) is used. The basic operation of the optimization process is minimizing of the functional built from both experimental results and numerical simulation and characterizing the difference between them. This functional £ depends on the vector of the parameters $\underline{C}$ and can be

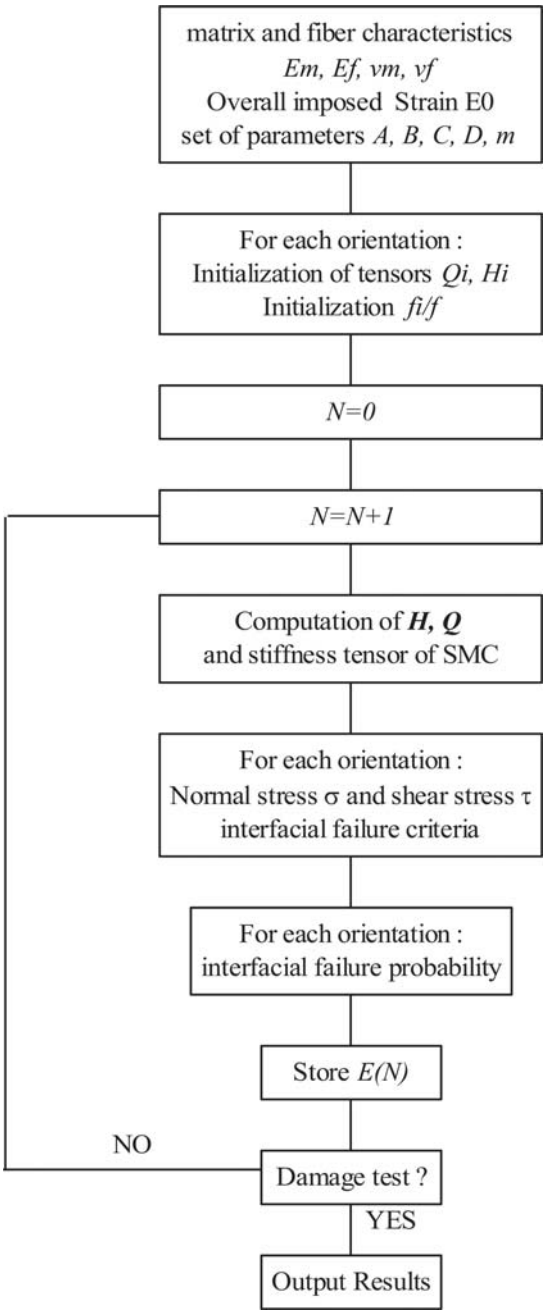

Fig. 5 General scheme for proposed methodology

expressed as the sum of elementary functional $£_k$, defined for each test (k) in experimental base:

$$£(\underline{C}) = \sum_k £_k(\underline{C}) \quad \text{(Eq 12)}$$

$$£_k(\underline{C}) = \frac{1}{N_k}\sum_{j=1}^{N_k}[Z_j^{k*} - Z_j^k][D][Z_j^{k*} - Z_j^k] \quad \text{(Eq 13)}$$

A "test" is either a true measurement or a set of required values, to be reached by the design (e.g., a prescribed stress level at given points). The expression of $£_k$ is given in the space of "observable" variables, which are "measured" during the test (k), at N_k sampling points: $\boldsymbol{Z}_j^k$ is the vector of the experi-

mental values, obtained as a response to the applied solicitation at the measurement location (and/or time) j: $\mathbf{Z}_j^{k*}$ denotes the simulated response, depending on $\underline{C}$, at some points. The matrix [**D**] is diagonal and allows a balance between the points, for instance, to increase the weight of the most precise measurements. As classically known, functionals are often badly conditioned (minima in narrow and elongated zones, existence of local minima, etc.), so that the simultaneous contribution of several minimization algorithms is needed. In the present case, the minimization technique used for the solution of the nonlinear optimization problem associates a gradient method and modified Newton-Raphson method for accelerating the convergence rate in the final phase of the identification. Evaluation of the gradient is made numerically by perturbation: the fact that no analytical evaluation is needed makes its use simple for any type of model.

Two principal methods can be used in an optimization procedure:

- The first one is based on the sensitivity analysis in which the partial derivative of the physical variables in relation to the optimizing parameters is used. These values can be numerically or analytically evaluated and implemented in the simulation code.
- The second approach, used by Pilvin et al. (Ref 29, 30) and adopted in the present work, is based on the evaluation of the derivative form by perturbation using two different processes: the SIDOLO code is the "master," and the damage code is the "slave." The function of the slave code is to predict the evolution of Young's modulus with the number of cycles. The modular aspect of this method offers to the user the opportunity of modifying the calculation of the cost function so that the type of optimization described above can be achieved using a similar scheme.

In our present optimization, the components of vector $\underline{C}$ are the material parameters used in the interfacial failure criterion:

$$\underline{C} = (m, A, B, C, D) \tag{14}$$

Compared with Eq 12 and 13, four tests are considered. For each one, the elementary functional is given by:

$$£_k(\underline{C}) = \sum_{j=1}^{N} [E^*(j) - E(j)]^2 \tag{15}$$

where $E^*(j)$ and $E(j)$ are respectively the values of the simulated and experimental values of Young's modulus after j cycles.

Figure 6(a)-(d), respectively, show a comparison between simulated stiffness reduction and experimental stiffness reduction for the four imposed strain levels ($\Delta\varepsilon_1 = 0.60\%$, $\Delta\varepsilon_2 = 0.72\%$, $\Delta\varepsilon_3 = 0.80\%$, $\Delta\varepsilon_4 = 0.87\%$). The predicted Young's modulus reduction agrees well with experimental observations. An optimal parameter set is given in Table 2.

For monotone loading ($N = 0$), the ratios A/B (for normal stress) and C/D (for shear stress) are equal to 17 and 9 MPa, respectively. These values correspond, respectively, to the interface strength in the normal and tangential directions.

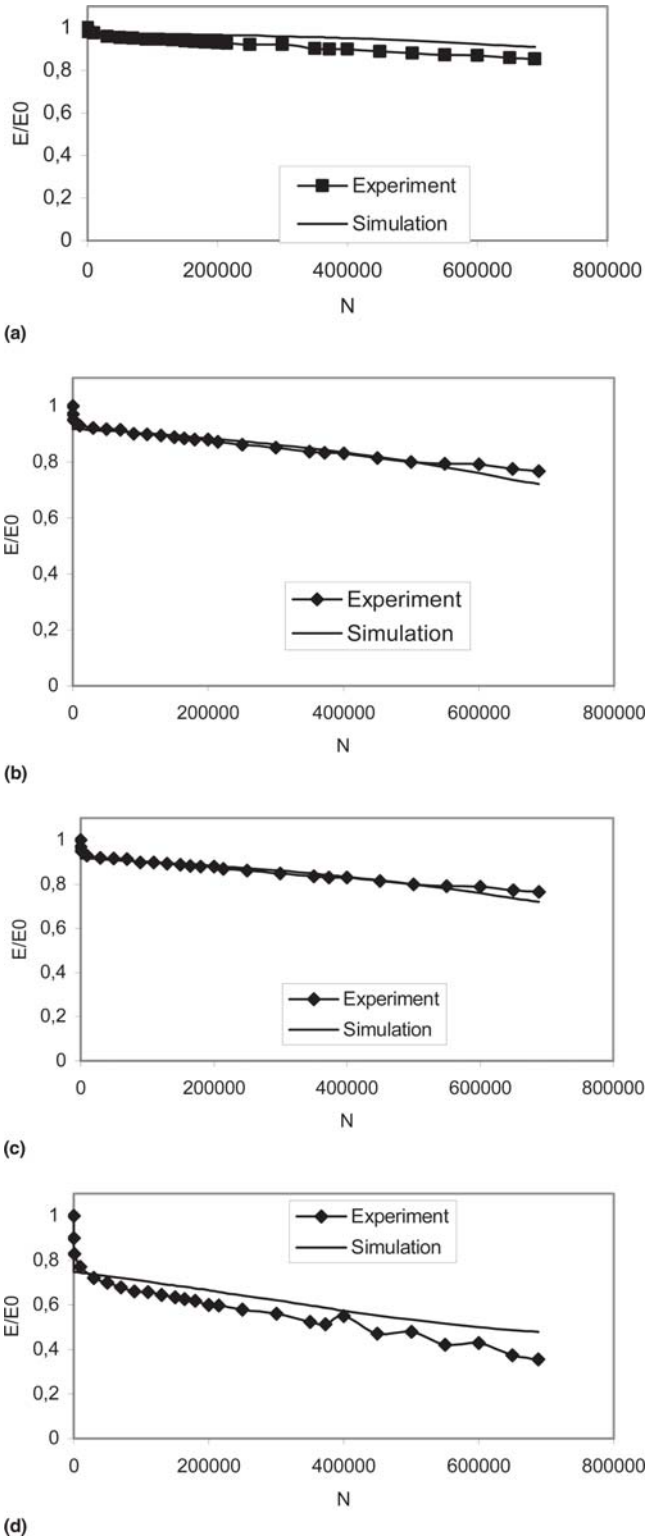

Fig. 6 Evolution of stiffness reduction with number of cycles: (a) $\varepsilon = 0.60\%$, (b) $\varepsilon = 0.72\%$, (c) $\varepsilon = 0.80\%$, (d) $\varepsilon = 0.87\%$

Table 2 Optimal parameter values

Parameter	*A*	*B*	*C*	*D*	*m*
Optimal value	2.4×10^5	0.143×10^5	21×10^5	2.21×10^5	0.21

4. Conclusions

In the SMC material studied herein, the dominant damage mechanism is interfacial decohesion, which leads to degradation of the mechanical properties, i.e., reduction in stiffness. A formulation of a micromechanical damage constitutive model is presented to predict stiffness reduction as a function of the number of fatigue cycles. This model is based on a quadratic interfacial criterion expressed in terms of normal and shear local stresses at the fiber-matrix interface.

To assess the model ability, four tests are considered in the experimental data set. It was shown to be possible to obtain a good correlation with a set of results including various strain ranges.

The complete parameter set in the model can be easily determined, thanks to the modular form of SIDOLO. An accelerated procedure is also used to avoid cycle-per-cycle computations.

This micromechanical model allows prediction of the complete damage elastic behavior law of an SMC composite as a function of the microstructure parameters. The local interface damage law introduced in the Mori-Tanaka model leads to the prediction of the hysteresis stress strain loop in fatigue. It can be used for a three-dimensional applied stress or strain tensor. It predicts the evolution of the mechanical properties with the number of cycles due to damage.

References

1. D.L. Denton, *The Mechanical Properties of an SMC R50 Composite,* Owens Corning Fiber Glass Corporation, Granville, OH, 1979
2. S.K. Chaturverdi, C.T. Sun, and R. Lsierakowski, Mechanical Characterization of Sheet Moulding Compound Composites, *Polym. Compos.,* 1983, **3,** p 167-171
3. M. Maalej, V.C. Li, and T. Hashida, Effect of Fiber Rupture on Tensile Properties of Short Fiber Composites, *J. Eng. Mech.,* 1995, **121,** p 903-913
4. Y.H. Zhao and G.J. Weng, A Theory of Inclusion Debonding and Its Influence on the Stress-Strain Relation of a Ductile Matrix Composite, *Int. J. Damage Mech.,* 1995, **4,** p 196-211
5. Y.H. Zhao and G.J. Weng, Plasticity of a Two-Phase Composite with Partially Debonded Inclusions, *Int. J. Plast.,* 1996, **12,** p 781-804
6. T. Watanabe and M. Yasuda, Fracture Behaviour of Sheet Moulding Compound, Part 1: Under Tensile Load, *Composites,* 1982, **13**(1), p 54-58
7. T. Watanabe and M. Yasuda, Fracture Behaviour of Sheet Moulding Compound, Part 2: Influence of Constituents on Mechanical Properties, *Composites,* 1982, **13,** p 59-65
8. J.F. Mandell and B.L. Lee, Matrix Cracking in Short Fiber Static and Fatigue Loading, *Proc. 6th Conf. Composite Materials, Testing and Design,* I.M. Daniels, Ed., ASTM, 1982, p 200-222
9. J.E. Lindhagen and L.A. Berlund, Application of Bridging-Law Concepts to Short-Fibre Composites, Part 2: Notch Sensitivity, *Compos. Sci. Technol.,* 2000, **60,** p 885-893
10. K. Togho and G.J. Weng, A Progress Damage Mechanics in Particle-Reinforced Metal Matrix Composites under High Triaxial Tension, *J. Eng. Mater. Technol.,* 1994, **116,** p 414-420
11. J.W. Ju and H.K. Lee, A Micromechanical Damage Model of Effective Elastoplastic Behaviour of Ductile Matrix Composites Considering Evolutionary Complete Particle Debonding, *J. Comput. Methods Appl. Mech. Eng.,* 2000, **183,** p 201-222
12. J.W. Ju and T.M. Chen, Micromechanics and Effective Moduli of Elastic Composites Containing Randomly Dispersed Inhomogeneities, *Acta Mech.,* 1994, **103,** p 103-121
13. J. Kabelka, L. Hoffman, and G.W. Ehrenstein, Damage Process Modeling on SMC, *J. Appl. Polym. Sci.,* 1996, **62,** p 181-198
14. F. Meraghni, C.J. Blakeman, and M.L. Benzaghagh, Effect of Interfacial Decohesion on Stiffness Reduction in a Random Discontinuous Fiber Composite Containing Matrix Microcracks, *Compos. Sci. Technol.,* 1996, **56,** p 541-555
15. H.K. Lee and S. Simunovic, A Damage Constitutive Model of Progressive Debonding in Aligned Discontinuous Fiber Composites, *Int. J Solid Struct.,* 2001, **38,** p 875-895
16. M. Maalej, Tensile Properties of Short Fiber Composites with Strength Distribution, *J. Mater. Sci.,* 2001, **26,** p 2203-2212
17. G. Guo, J. Fitoussi, and D. Baptiste, A Sequential and Biaxial Tensile Loading Test to Investigate the Damage Behaviour in a Random Short Fiber SMC Composite, *Anal. Compos. AMAC,* 1995, **3,** p 41-42
18. G. Guo, J. Fitoussi, and D. Baptiste, Optimisation of a Failure Criterion for the Short-Fiber Reinforced Composites Materials by the Finite Element Analysis Using a Damage Micromechanics Model, *Progress in Advanced Materials and Mechanics,* Peking University Press, 1996, p 675-687
19. G. Guo, J. Fitoussi, and D. Baptiste, Extension of Successive Iteration Method in the Homogenization of a Random Short-Fiber Reinforced Composite, *Microstructures and Mechanical Properties of New Engineering Materials, Proc. 2nd IMMM'95,* International Academic Publishers, 1995, p 15-21
20. G. Guo, J. Fitoussi, and D. Baptiste, Determination of Tridimensional Failure Criterion at the Fiber/Matrix Interface at an Organic Matrix and Discontinuous Reinforced Composite, *JNC9,* J.P. Favre and A. Vaurin, Ed, AMAC, St. Etienne, France, 1994, p 213-222
21. K. Derrien, J. Fitoussi, and D. Baptiste, Prediction of the Effective Damage Properties and Failure Properties of Nonlinear Anisotropic Discontinuous Reinforced Composites, *Comput. Methods Appl. Mech. Eng.,* 2000, **185,** p 93-107
22. E. Le Pen, D. Baptiste, and G. Hug, Multi-scale Fatigue Behaviour Modelling of Al-Al_2O_3 Short Fibre Composites, *Int. J. Fatigue,* 2002, **24,** p 205-214
23. P.M. Lesne and S. Savalle, An Efficient Cycles Jump Technique for Viscoplastic Structure Calculations Involving Large Number of Cycles, *Proc. 2nd Int. Conf. on Computational Plasticity* (Barcelona), 1989, p 591-602
24. T. Keyvani, "Contribution à la Caractérisation Micromécanique et Ultrasonore du Comportement et de l'Endommagement des Composites de Type SMC (Sheet Moulding Compound)," PhD Thesis, l'Ecole Centrale Paris, 1992
25. T. Mori and K. Tanaka, Average Stress in Matrix and Average Elastic Energy of Materials with Misfitting Inclusions, *Acta Metallurgica,* 1973, **21,** p 547-574
26. J.D. Eshelby, Elastic Inclusion and Inhomogeneities, *Progress in Solid Mechanics,* North Holland Publishing, 1961, p 87-140
27. J.D. Eshelby, The Determination of Elastic Field of an Ellipsoidal Inclusion, and Related Problems, *Proc. R. Soc. London,* 1957, **A241,** p 376-396
28. P. Pilvin, Identification des Paramètres de Modèles de Comportement, *Proc. Mecamat: Inelastic Behaviour of Solids,* Aug. 30 to Sept. 1 (Besançon, France), 1988
29. P. Pilvin, K. Saï, and G. Cailletaud, Optimal Design against Creep and Fatigue, *Proc. 4th Int. Conf. on Nonlinear Engineering Computations,* N. Bicanic, P. Marovic, D.R.J. Owen, V. Jovic, and A. Mihanovic, Ed., Sept. 16-20, 1991 (Swansea), p 731-740
30. P. Pilvin, K. Saï, G. Cailletaud, "Shape and Material Optimization in Cyclic Plasticity," Int. Conf. on Computational Plasticity, April 1992 (Barcelona, Spain)